Dissecting the Catalytic Mechanism of Staphylococcal Lipases Using Carbamate Substrates: Chain Length Selectivity, Interfacial Activation, and Cofactor Dependence†

Jan-Willem F. A. Simons, Jan-Willem P. Boots,‡ Mark P. Kats, Arend J. Slotboom, Maarten R. Egmond, and Hubertus M. Verheij*

Department of Enzymology and Protein Engineering, CBLE, Utrecht University, The Netherlands

Received June 9, 1997; Revised Manuscript Received August 26, 1997⊗

ABSTRACT: *p*-Nitrophenyl *N*-alkylcarbamates with different alkyl chains were used as substrates to determine separately the carbamylation and decarbamylation rates of the lipases from *Staphylococcus hyicus* and *S. aureus*. Both enzymes are reversibly inhibited by these compounds due to a rapid carbamylation of their active site serines followed by a slow decarbamylation. The carbamylation reaction is strongly pH-dependent and the pH profile suggests that an unprotonated histidine is required for this reaction. In contrast, the decarbamylation is pH-independent suggesting the presence of a hydrogen bond between the active site histidine and the carbamyl moiety. *S. hyicus* lipase preferably reacts with medium to long chain carbamates with an optimum for eight carbon atoms. In contrast, *S. aureus* lipase is highly specific for short chain carbamates. These results are in agreement with the respective substrate preferences of both lipases toward natural lipids. The decarbamylation rates of both enzymes hardly depend on the alkyl chain length, and from this it is concluded that chain length selectivity is expressed in the first step of catalysis. Both the carbamylation and decarbamylation reaction rates of *S. hyicus* lipase are enhanced in the presence of micelles, the activation effect being most pronounced in the first step. For the *S. aureus* lipase only a small influence of interfaces on both reaction steps was observed. These results are discussed in view of a possible role of a lid covering the active site. Kinetic experiments in the presence and absence of calcium strongly suggest that calcium ions are important for the structural stabilization of the unmodified as well as of the carbamylated enzymes. This structural function of calcium was supported by urea unfolding experiments, from which it appeared that for both enzymes the free energy for unfolding is significantly lower in the absence of calcium. In conclusion our results show that the kinetic differences between both lipases reside in the acylation step, and that calcium is important for the structural stabilization of the unmodified, and moreover, the acylated enzymes.

Lipases (EC 3.1.1.3) are specialized to hydrolyze under physiological conditions the ester bonds present in long chain triacylglycerols (*1*). Because of the low solubility of these compounds in an aqueous environment, lipases are active under extraordinary conditions as compared to other water-soluble enzymes and encounter their substrate at a lipid−water interface formed by oil droplets, (mixed) micelles or bilayer structures. Consequently, one of the central themes in interfacial enzyme kinetics is the phenomenon of activation at a substrate interface, which was experimentally demonstrated for the first time for porcine pancreatic lipase in the classical experiments of Sarda and Desnuelle (*2*). After the appearance of this pioneering paper, several authors observed similar effects with many other lipolytic enzymes. The kinetics of lipolytic enzymes at the interface have been described in detail by Verger and de Haas (*3*), and a model is depicted in Scheme 1. According to this model lipases can hydrolyze monomeric substrate molecules, but only after binding to the interface conversion of aggregated substrate can take place. This initial binding step of the lipase to the substrate interface, followed by binding of a single substrate molecule in the active site of the enzyme and catalytic turnover, results in complex kinetics as compared to the situation where both enzyme and substrate are water-soluble.

Several models have been proposed to explain the so-called "interfacial activation" of lipolytic enzymes, and these models have been grouped into substrate models and enzyme models (*4*). In the substrate models it is assumed that the lipids in the aggregate are in an optimal orientation, conformation, and/or hydration state for enzymatic breakdown. A common feature of all substrate models is that the enzyme is thought to be structurally invariant, both in the absence and in the presence of a substrate interface. In the enzyme models it is thought that the enzyme undergoes conformational rearrangements leading to an optimized active site geometry and enhanced catalytic activity.

After the enzyme models were proposed, it took years before structural proof supporting these models was obtained. Only recently NMR solution structures of free and micelle-bound porcine pancreatic phospholipase A_2 (PLA_2)[1] demonstrated that minor, but important structural changes at the N-terminus take place that optimize the active site for catalysis and result in a strongly enhanced activity (*5*). Also

† This research was carried out with financial aid from the BRIDGE-T-lipase program of the European Communities under Contract N-BIOT-0194 NL, the Biotech-G-lipase program under Contract BIO2 CT94-3013, and the Dutch Foundation for Chemical Research (SON).

* Author to whom correspondence should be addressed at the Department of Enzymology and Protein Engineering, CBLE, Utrecht University, Padualaan 8, P.O. Box 80054, NL-3508 TB Utrecht, The Netherlands. FAX: +31-30-2522478.

‡ Present address: Department of Biochemistry of Biomembranes, CBLE, Utrecht University.

⊗ Abstract published in *Advance ACS Abstracts,* November 1, 1997.

S0006-2960(97)01371-8 CCC: $14.00

Scheme 1: Model for the Action of Lipases at an Interface[a]

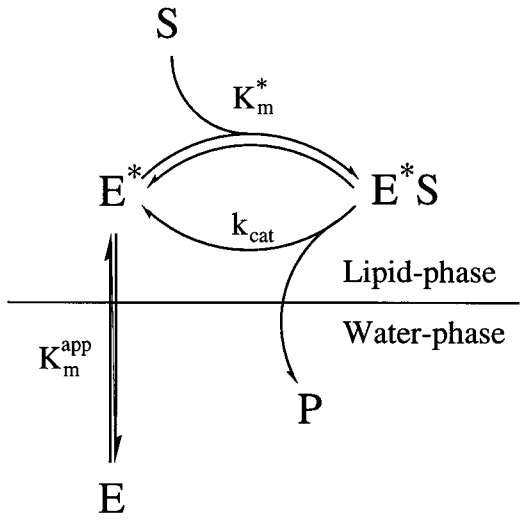

[a] The following symbols are used: E, enzyme in water phase; E*, enzyme adsorbed to the interface; S, substrate; E*·S, interfacial enzyme−substrate complex; K_m^{app}, apparent three-dimensional affinity constant; K_m^* interfacial (two-dimensional) affinity constant; k_{cat}, catalytic rate constant; P, products of hydrolysis [model adapted from Verger and de Haas (*3*)]. Note that the enzymatic conversion of substrate into products (E*S → E*+P) is represented as a one-step process for reasons of simplicity.

for lipases structural information was obtained only recently. The X-ray structure of human pancreatic lipase (*6*) contains an active site which is blocked by large surface loops. These loops prevent substrate molecules from reaching the active site, and the authors suggested that important structural rearrangements have to take place before substrate molecules can enter. The X-ray structure of human pancreatic lipase in the presence of its cofactor colipase and mixed phospholipid/detergent micelles revealed that such structural rearrangements indeed take place upon binding to a substrate interface (*7*). The predominant change is the displacement of the surface loop which blocks the entrance to the active site, in literature often referred to as the "lid" or the "flap", thereby making the active site triad accessible for substrate molecules. Furthermore, rearrangements take place that result in an optimization of the oxyanion hole.

This information at the molecular level provided a structural basis for the observed enhancement of activity of pancreatic lipases at the substrate interface. The induction of such conformational changes is not restricted to the presence of an interface, since they were also reported for lipases that have an inhibitor covalently bound in the active site (*8*,*9*). The inhibitors were small organophosphates or *n*-alkylsulfonates mimicking the transition state of acyl enzyme hydrolysis and *O*-methylhexylphosphonate which might be considered as an analogue mimicking the transition state of substrate hydrolysis (*10*). These observations suggest that not only binding to a substrate interface but also binding of a substrate molecule into the active site can induce conformational changes of lipases resulting in the "activated form".

Proteins or enzymes with a comparable structure that display differences in biochemical properties are useful tools to elucidate structure−function relationships. An example is the lipase isolated from guinea pig pancreas (*11*). This enzyme has a smaller lid than the homologous human pancreatic lipase, and it was suggested that this is the structural basis for the observation that guinea pig lipase does not display interfacial activation. Another example of a protein that illustrates the usefulness of two highly similar enzymes are the lipases I and II (85% sequence identity) isolated from *Geotrichum candidum*. Although these lipases have an almost identical three-dimensional structure, lipase I has a high preference for *cis*-Δ9-unsaturated long chain fatty acids whereas lipase II has a much broader specificity (*12*). Subtle structural differences are probably responsible for this selectivity in fatty acid profile (*13*). Both the study with the mammalian pancreatic lipase couple and the fungal lipase couple have contributed to a better understanding of differences in lipase substrate selectivity and also to the physiological importance of these differences.

Recently, we reported the purification and characterisation of two highly similar lipases from bacterial origin (*14*). The lipase from *Staphylococcus hyicus* (SHL) degrades both short and long chain triacylglycerols and in addition has a high activity toward phospholipids. In contrast, the *S. aureus* lipase (SAL) degrades only short chain lipids and is inactive toward phospholipids. In view of this difference in specificity and because of the fact that both enzymes need calcium for full catalytic activity, it is unlikely that calcium ions are only involved in the binding of phospholipids. On the basis of inhibition studies with hexadecylsulfonyl fluoride, Leuveling Tjeenk and co-workers concluded that calcium might be involved in SHL stability (*15*). The precise role of calcium, however, is not yet known. Also the structural basis for the differences in substrate and chain length selectivity between SHL and SAL are not understood. In an attempt to find answers to these questions and to study the influence of interfaces on kinetics, we decided to make use of *p*-nitrophenyl *N*-alkylcarbamates of different chain length. Carbamates have been used successfully as substrate analogs to shed light on the kinetic behavior of esterases, proteases, and lipoprotein lipase (*16*−*20*). These studies showed that these compounds are poor substrates that act as inhibitors by reversible carbamylation of the active site serine.

We synthesized *p*-nitrophenyl *N*-alkylcarbamates with different alkyl chains to study the remarkable difference in chain length selectivity between SHL and SAL. Here we report the kinetics of carbamylation and decarbamylation of SHL and SAL in relation to the hydrolysis of *p*-nitrophenyl butyrate as a substrate. Using this approach we studied the influence of interfaces on the rates of both steps of catalysis. Moreover, we show that carbamates can be used to investigate the influence of calcium ions on both carbamylation and decarbamylation steps.

MATERIALS AND METHODS

Chemicals. *p*-Nitrophenyl butyrate (PNPB) was purchased from Sigma. *n*-Octyl-poly-oxyethyleneglycol (OPOE), tau-

[1] Abbreviations: BSA, bovine serum albumin; BSF, butylsulfonyl fluoride; CMC, critical micelle concentration; EDTA, *N*,*N*,*N*,*N*-ethylenediaminetetraacetic acid; PNPB, *p*-nitrophenyl butyrate; PNPBC, *p*-nitrophenyl *N*-butylcarbamate; PNPDC, *p*-nitrophenyl *N*-dodecylcarbamate; PNPEC, *p*-nitrophenyl *N*-ethylcarbamate; PNPOC, *p*-nitrophenyl *N*-octylcarbamate; PLA_2, porcine pancreatic phospholipase A_2; SAL, *Staphylococcus aureus* lipase; SHL, *Staphylococcus hyicus* lipase; BC-SAL and BC-SHL, SAL and SHL after inhibition with PNPBC; BS-SAL and BS-SHL, SAL and SHL after inhibition with BSF; $C_{18:1}$-PN, *n*-oleylphosphocholine; OPOE, *n*-octyl-poly-oxyethyleneglycol; TDOC, taurodeoxycholic acid; TX100, Triton X-100.

rodeoxycholic acid (TDOC), and Triton X-100 (TX100) were from Alexis Corporation, Sigma and Serva, respectively. *n*-Oleylphosphocholine ($C_{18:1}$-PN) was synthesized analogous to C_{16}-PN (*21*). Bovine serum albumin (BSA) was obtained from Boehringer. *N,N,N,N*-Ethylenediaminetetraacetic acid (EDTA) was purchased from Acros Chimica. *p*-Nitrophenyl chloroformate, butylamine, dodecylamine, ethylamine, and octylamine were from Sigma. Butylsulfonyl fluoride (BSF) was prepared from the corresponding chloride analoguous to hexadecylsulfonyl fluoride (*22*). Small-scale gel filtration PD-10 columns (Sephadex G-25) were purchased from Pharmacia.

Enzymes. Recombinant histidine-tagged SHL and SAL were isolated from *Escherichia coli* by affinity chromatography on nickel-nitrilotriacetic acid as described before (*14*). The presence of a short N-terminal extension containing six successive histidines does not alter the kinetic properties of these enzymes as compared to the wild-type forms. Protein concentrations were determined by measuring the absorbance at 280 nm using calculated $E^{1\%}_{280nm}$ values of 14.5 for SHL and 15.8 for SAL (*23*).

Synthesis of Carbamate Inhibitors. The *p*-nitrophenyl *N*-ethyl, -butyl, -octyl, and -dodecyl carbamates (PNPEC, PNPBC, PNPOC, and PNPDC) were synthesised from their respective *n*-alkylamine and *p*-nitrophenyl chloroformate essentially as described before (*19,20*). The crude products were purified by column chromatography using silicic acid gel followed by crystallization from diethylether/hexane at 4 °C. The identity and purity of the carbamates were checked by determination of their melting points and by TLC, proton NMR, and mass spectrometry.

Determination of Concentration, Solubility, and Stability of Carbamates. Stock solutions of carbamates were prepared in acetonitrile by dissolving weighted amounts of dry powder. The concentration of *p*-nitrophenyl carbamate was then checked spectrophotometrically as follows. An aliquot of the stock solution was hydrolysed for 24 h in 5 M sodium hydroxide. This solution was diluted 10-fold, and the absorbance was measured at 348 nm, which is the isosbestic point of the *p*-nitrophenol/*p*-nitrophenolate couple. From this absorbance the concentration of liberated *p*-nitrophenol/*p*-nitrophenolate was calculated using a molar absorption coefficient of 5150 M^{-1} cm^{-1} (*24*). To determine the solubility of the carbamates, an aliquot of the concentrated stock solution in acetonitrile was diluted 25-fold in 50 mM Hepes, pH 7 containing 10 mM $CaCl_2$ and 0.5 mg/mL BSA. After centrifugation (14000*g*, 10 min) the concentration of carbamate in the supernatant was determined as described above. The stability of the carbamates was determined by diluting an aliquot of the carbamate stock solution into 1 mL of 50 mM Hepes at pH 7. The increase in absorbance at 348 nm was followed in time, and the first-order rate constant for basic hydrolysis, k_h, was calculated by fitting the data to the equation

$$A_t = A_o \exp(-k_h t) \qquad (1)$$

In this equation A_t and A_o are absorbances at 348 nm at times t and 0, respectively.

Enzyme Activity Assays. The enzymatic activity of SHL and SAL with monomeric PNPB as a substrate was routinely determined by following the increase in absorbance at 400 nm due to the release of *p*-nitrophenol. For activity calculations a pK_a of 7 for *p*-nitrophenol and an extinction coefficient of 18577 M^{-1} cm^{-1} for *p*-nitrophenolate were used. This assay contained 250 μM PNPB, 50 mM Hepes, pH 7, and 10 mM $CaCl_2$ in a total volume of 1 mL. The reaction temperature was 18 °C, and the spectrophotometer used was a Pharmacia LKB-Ultrospec III or a Shimadzu UV-150-02. In this assay the activities of SHL and SAL are 75 and 14 units/mg, respectively. To obtain specificity constants (k_{cat}/K_M) the activity was determined at PNPB concentrations between 0 and 1 mM. The solubility limit of PNPB is 1.1 mM under these conditions. For both SHL and SAL a linear relationship between activity and [PNPB] was found, from which the specificity constants were calculated. To obtain the pH−activity profile of both lipases with PNPB as a substrate the following buffers were used: formate (pH 3 and 3.5), acetate (pH 4 up to 5.5), succinate (pH 6 and 6.5), Hepes (pH 7 and 7.5), and Tris/HCl (pH 8 and 8.5), all at concentrations of 50 mM. The increase in absorbance was followed at the isosbestic point, and the activities were calculated using an absorption coefficient of 5150 M^{-1} cm^{-1}.

Carbamylation Kinetics. To determine the carbamylation rate constants of SHL and SAL two types of inhibition experiments were used: a discontinuous approach and a continuous approach. In the discontinuous approach the enzyme was incubated in the presence of at least a 10-fold molar excess of carbamate over enzyme in a total volume of 500 μL. Unless otherwise stated, the inhibition mixture contained 50 mM Hepes, pH 7, 10 mM $CaCl_2$, and 0.5 mg/mL BSA at 18 °C. BSA was included to prevent adsorption of the lipase to the cuvette wall, while it does not influence the enzymatic activity of the lipase. The carbamate was added from a concentrated stock in acetonitrile; the final volume fraction of acetonitrile in the mixture never exceeded 0.04. At regular time intervals an aliquot was taken to determine the remaining activity in the PNPB assay. From the resulting data the pseudo-first-order rate constant for carbamylation (k_c^{obs}) was obtained as follows.

For the carbamylation reaction as depicted in Scheme 2 the first equilibrium is fast relative to the carbamylation step k_c. Since k_1 and k_2 were not obtained independently, their ratio K_C (= k_2/k_1) is used in the calculations below. When we define $k_c^{obs} = k_c C/K_C + C$, where C is the concentration of carbamate present, we can write the rate equation (eq 2) for the carbamylation/decarbamylation reaction:

$$d(EC)/dt = k_c^{obs} E_0 - (k_c^{obs} + k_d)(EC) \qquad (2)$$

where E_0 and EC represent total enzyme and carbamylated enzyme concentrations, respectively. Because carbamate concentrations (C) were always in excess over enzyme present (E_0), the amount of C bound to the enzyme was neglected in the calculations discussed below. Equation 2 can be integrated when the carbamate concentration (C) remains approximately constant during the carbamylation reaction. We then obtain

$$(EC)_t = k_c^{obs} E_o(1 - \exp[-(k_c^{obs} + k_d)t])/(k_c^{obs} + k_d) \qquad (3)$$

This equation predicts that the carbamylation reaction relaxes to a plateau value for (EC) at infinite time. From this plateau value the ratio of the carbamylation and decarbamylation rate constants (i.e. k_c^{obs}/k_d) can be found. Fitting experimental relaxation data to eq 3 by nonlinear regression methods also

Table 1: Solubility and Stability of Carbamates Used in this Study[a]

carbamate	solubility (μM)	$10^4\ k_h$ (s^{-1})	$t_{1/2}$ (min)
PNPEC	1600	1.65	70
PNPBC	200	1.05	110
PNPOC	40	*b*	*b*
PNPDC	10	*b*	*b*

[a] Solubility and stability were determined in 50 mM Hepes, pH 7, at 18 °C. The stability is represented as the first-order rate constant obtained by fitting to eq 1 (k_h) and for reasons of clarity the half-life time ($t_{1/2}$) in minutes is given as well. Further details are described in Materials and Methods. [b] Upon incubation for 8 h at pH 7 less than 5% of the maximum release of *p*-nitrophenol was observed.

allowed us to obtain values for ($k_c^{obs} + k_d$) from the exponential term, thereby yielding values for k_c^{obs} and k_d separately. When carbamylation experiments are repeated for different carbamate concentrations, the constants k_c and K_C can be derived from $k_c^{obs} = k_c C/K_C + C$. It was noted that a plateau is not always reached, particularly when carbamylation reactions were relatively slow (see e.g. Figure 2). Such behavior is only observed when the carbamate concentration *C* drops during the carbamylation reaction due to nonenzymatic hydrolysis. In that case integration of eq 2 is not allowed. Indeed it was noted that several carbamates are slowly hydrolyzed nonenzymatically under our conditions (see data in Table 1). Therefore, enzymatic carbamylation data were collected only for those conditions where the drop in carbamate concentration (*C*) is negligible. Using eq 2 and the half-life times of the carbamates it was verified whether this was allowed under our experimental conditions.

In the continuous approach the carbamylation rate constant was determined in the presence of substrate, essentially as described by Hosie *et al.* (*25*). These experiments were performed in a total volume of 3 mL containing 500 μM PNPB, 50 mM Hepes, pH 7, and 10 mM $CaCl_2$ and different concentrations of carbamate which were varied between 0 and 10 μM. When these experiments were performed in the presence of 100 mM TX100, the PNPB concentration was 2 mM and the carbamate concentration was varied between 0 and 60 μM. For these experiments a double beam Varian Cary 04E UV/vis spectrophotometer interfaced to an IBM personal computer for data collection was used. The reaction was started by adding SHL at a concentration of 5.5 nM to the cuvette. At this low enzyme concentration, the release of *p*-nitrophenol resulting from carbamylation is negligible compared to *p*-nitrophenol released by PNPB hydrolysis. In the absence of carbamate the slope was constant for at least 10 min. When the experiment was repeated in the presence of inhibitor the slope of the curve decreased with time and at regular time intervals the first order derivative of the curve was calculated and divided by the value obtained without inhibitor. From the remaining activities the first order carbamylation rate constant was calculated by fitting the data to eq 3.

Preparative Carbamylation and Isolation of Carbamylated Enzyme. Preparative carbamylation was done using an enzyme concentration of 5 μM for SHL or 10 μM for SAL in a total volume of 2.5 mL containing 50 mM Hepes, pH 7, 10 mM $CaCl_2$, and one of the carbamates PNPEC (1.6 mM), PNPBC (200 μM), PNPOC (40 μM), or PNPDC (10 μM). The enzymatic activity was followed in time in the PNPB assay as described above. When the lowest activity was reached, the reaction mixture was passed over a PD-10 column equilibrated in water to remove excess unreacted carbamate, formed *p*-nitrophenol and carbamic acid, Hepes and $CaCl_2$. The absence of unreacted carbamate after the PD-10 column was verified by dilution of an aliquot in 5 M sodium hydroxide and measuring the absorbance at 400 nm. The concentration of eluted protein was determined spectrophotometrically at 280 nm. The carbamyl-enzyme was divided into aliquots which were stored at −20 °C. Under these conditions a slow decarbamylation occurs, but when used within 5 days the percentage of free enzyme never exceeded 15%.

Decarbamylation Kinetics. To determine rate constants of decarbamylation, a fraction of 50 μL of carbamylated enzyme was thawed and the total volume was diluted to 500 μL with Hepes buffer (50 mM) containing 10 mM $CaCl_2$ and 0.5 mg/mL BSA at pH 7. This resulted in a concentration of carbamylated enzyme of approximately 0.25 μM for SHL and 0.5 μM for SAL. To study the influence of an interface and the cofactor calcium on the decarbamylation, incubations were done in the presence of different detergents or 10 mM solutions of EDTA, calcium, strontium, or barium. The decarbamylation reaction was followed by taking aliquots at regular time intervals and measuring the activities in the PNPB assay. The percentage of carbamylated enzyme at each time point was determined by calculating the concentration of active enzyme from the measured activity and subtracting this value from the total enzyme concentration (carbamylated and non-carbamylated) which was determined spectrophotometrically. Subsequently the first-order rate constant for decarbamylation was calculated from these data.

Preparation of Sulfonylated Enzymes. BS-SHL and BS-SAL were prepared by addition of 150 μL of 50 mM BSF, dissolved in acetonitrile, to 2.5 mL of 50 mM Hepes, pH 7, 10 mM $CaCl_2$ containing 25 μM of either SHL or SAL. Reactions were allowed to proceed for 24 h at room temperature, and then the reaction mixtures were applied to a PD-10 column, preequilibrated with 50 mM Hepes, pH 7, 1 mM $CaCl_2$, and 50 mM NaCl. The concentrations of the eluted, sulfonylated lipases were determined by measuring the absorbances at 280 nm. Experiments indicated no changes in molar absorptivities of both SHL and SAL on forming BS-SHL and BS-SAL. Less than 2.5% residual activity was detected in the sulfonylated preparations of both lipases by use of PNPB as a substrate. After the sulfonylation, BS-SHL and BS-SAL still migrated as one single band on SDS−PAGE gel electrophoresis (data not shown), demonstrating the purity of both preparations.

Urea Denaturation. The reversible folding of SHL, SAL, BS-SHL, and BS-SAL was monitored by fluorescence spectroscopy using a Perkin-Elmer LS-5 luminescence spectrophotometer (Perkin-Elmer, Beaconsfield, U.K.). The measurements were performed at 18 °C using an excitation wavelength of 280 nm while the emission was measured at 330 nm. Both slit widths were 5 nm. Two protein stock solutions were prepared, one containing folded and the other containing unfolded enzyme. The former solution contained 3 μM SHL or SAL, 50 mM Hepes, and either 10 mM $CaCl_2$ or 10 mM EDTA at pH 7.0, while the latter contained in addition 8 M urea to denature the protein. With each of these protein stock solutions a complete curve was measured. Thus the denaturation profile was determined by unfolding as well as refolding the protein. For unfolding experiments

Chart 1: Chemical Structures of Carbamates Used Compared to the Ester Substrate[a]

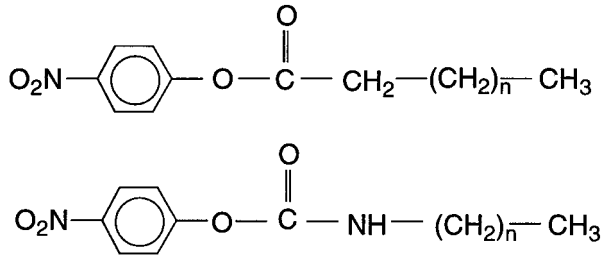

[a] Ester substrate: $n = 1$, *p*-nitrophenyl butyrate (PNPB). Carbamates: $n = 1$, *p*-nitrophenyl *N*-ethylcarbamate (PNPEC); $n = 3$, *p*-nitrophenyl *N*-butylcarbamate (PNPBC); $n = 7$, *p*-nitrophenyl *N*-octylcarbamate (PNPOC); $n = 11$, *p*-nitrophenyl *N*-dodecylcarbamate (PNPDC).

a sample of the solution containing folded enzyme was mixed with a buffer containing urea. The urea concentration was varied between 0 and 8 M. The same procedure was followed for refolding experiments using the solution containing unfolded enzyme. All samples were incubated for at least 15 min before measuring the fluorescence. For the unmodified as well as the sulfonylated lipases, the resulting unfolding and refolding profiles overlapped, indicating that each sample had reached equilibrium. The free energy of unfolding at each point of the denaturation profile was calculated using the equation

$$\Delta G_u = -RT \ln K_u \quad (4a)$$

where ΔG_u is the free energy of unfolding, R is the gas constant, T the absolute temperature, and K_u is the equilibrium constant for the unfolding reaction. The equilibrium constant K_u was calculated using the equation

$$K_u = (F_n - F_{obs})/(F_{obs} - F_u) \quad (4b)$$

where F_n, F_u, and F_{obs} represent the quantum yield of the native protein, the unfolded protein, and the observed quantum yield at that point of the denaturation profile, respectively. To obtain the free energy of unfolding in the absence of urea, ΔG_u was plotted versus the urea concentration and fitted to the equation

$$\Delta G_u = \Delta G_0 - m[\text{urea}] \quad (4c)$$

where ΔG_0 is is the free energy of unfolding in the absence of urea and m is the slope of the curve *(26)*.

RESULTS

We synthesized different *p*-nitrophenyl *N*-alkylcarbamates that are structurally similar to acyl *p*-nitrophenyl esters (Chart 1), but in which the methylene group adjacent to the ester function has been replaced by an amide function. This change makes the carbamate a poorer substrate than the ester. In addition, the introduction of the NH function increases the hydrophilicity of the carbamates compared to the esters. This is important since we intended to study the kinetics of lipases on monomeric and aggregated substrates, and therefore we determined the solubility of these carbamates under the assay conditions. The solubilities of different carbamates are given in Table 1. It is obvious that the water solubility decreases when chain length increases. With a solubility of 1.6 mM the ethyl carbamate PNPEC is about 1.5-fold more soluble than the isosteric butyric acid ester PNPB (Chart 1, $n = 1$). Furthermore, these carbamates are susceptible to spontaneous hydrolysis by water, and therefore we determined their stability in the absence of enzyme. With the rate constants given in Table 1 we were able to verify the obtained carbamylation rate constants taking into account this nonenzymatic hydrolysis (see Materials and Methods).

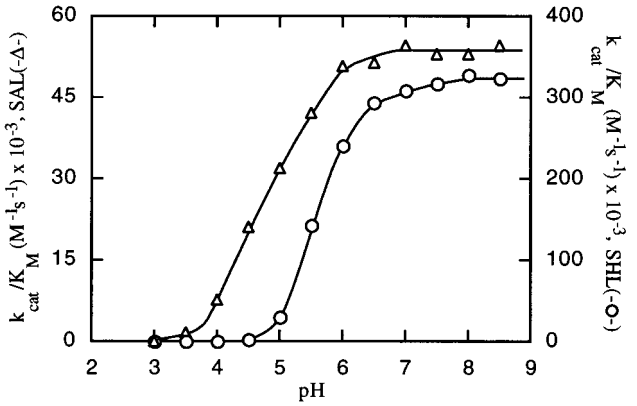

FIGURE 1: pH dependence of ester hydrolysis for SHL (○) and SAL (△) with PNPB as a substrate. Activities were determined in 50 mM buffer, 10 mM $CaCl_2$ at 18 °C. The substrate concentration was varied between 0 and 250 μM, and k_{cat}/K_M values were determined from the slopes of these curves as described in the text. Note the difference in scaling for the *Y*-axes.

Like most lipases both SHL and SAL can hydrolyze *p*-nitrophenyl acyl esters in the presence of TX100 *(14)*. Both SHL and SAL also rapidly hydrolyze monomeric PNPB and the reaction is linear with time without a burst. In the concentration range below 1.1 mM a linear increase in activity was observed with substrate concentration (data not shown). These experiments were carried out at varying pH values and from the slopes of the curves the specificity constants k_{cat}/K_m were determined. In Figure 1 the pH profiles of SHL and SAL with PNPB as a substrate are given. At a pH value of 7 or higher the catalytic efficiency of SHL is about 7-fold higher compared to SAL. The enzymatic activity of both enzymes strongly depends on pH resulting in sigmoidal curves. From the shapes of the curves it was concluded that a group with a pK_a of 5.0 controls the substrate hydrolysis by SAL whereas this value is 5.6 for SHL. With triacylglycerols as a substrate a similar difference in activity and a lower pH optimum for SAL compared to SHL has been observed *(14)*. Thus *p*-nitrophenyl esters may be used as substrate mimics for these lipases.

Initial experiments showed that under conditions where *p*-nitrophenyl esters are rapidly hydrolyzed, little or no hydrolysis occurred when SHL or SAL was added to a solution of PNPBC. Only when the amount of added enzymes was increased at least 100-fold was an initial burst of *p*-nitrophenol observed, but the rate of hydrolysis rapidly slowed down (data not shown). Such behavior can be explained by a slow carbamylation of the active site serine and an even slower decarbamylation (as depicted in Scheme 2), in analogy with the well-known acylation/deacylation that occurs in serine esterases. To investigate this reaction in more detail, SHL was incubated at pH 6.5 with an excess of PNPBC and at regular time intervals the remaining activity was determined. A typical curve of the enzymatic activity as well as the carbamate concentration, obtained in the presence of an initial concentration of 50 μM PNPBC, is

Scheme 2: Mechanism for Carbamylation and Decarbamylation of SHL and SAL[a]

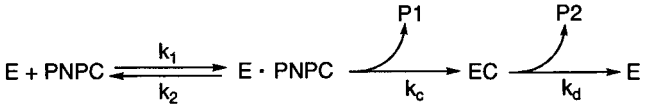

[a] The following symbols are used: E, enzyme; PNPC, *p*-nitrophenyl carbamate; E·PNPC, enzyme-*p*-nitrophenyl carbamate complex; EC, carbamylated enzyme; P_1, first product; P_2, second product; k_1, association rate constant for E·PNPC; k_2, dissociation rate constant for E·PNPC; k_c, carbamylation rate constant; k_d, decarbamylation rate constant.

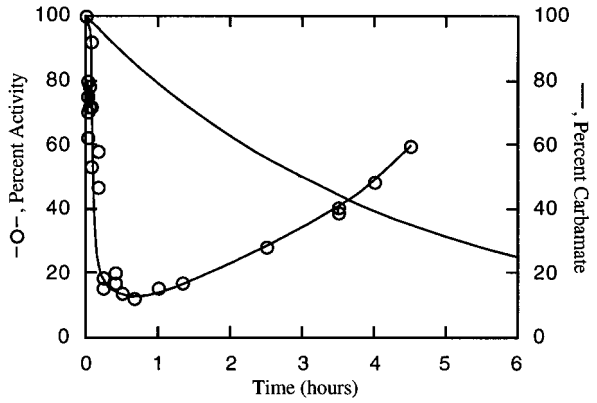

FIGURE 2: Inhibition of SHL with PNPBC. SHL (5 μM) was incubated with an initial concentration of 50 μM PNPBC in 50 mM succinate, pH 6.5, 10 mM $CaCl_2$ and 0.5 mg/mL BSA at 18 °C. Both the decrease in SHL activity (○) and the decrease in carbamate concentration due to nonenzymatic hydrolysis (−) are given. Percent remaining activities in time were determined with the discontinuous assay as described in Materials and Methods.

depicted in Figure 2. After an initial rapid decrease in activity, the residual activity levels off around a minimum value of 15−20%. Next, the activity slowly returns as a consequence of carbamate depletion due to nonenzymatic hydrolysis. At higher PNPBC concentrations the initial slope is steeper, the minimum activity is lower, and the regeneration of activity is slower (data not shown). Since upon incubation of SHL in the absence of carbamate no loss in activity was observed, even after 24 h, we concluded that inhibition was due to reversible carbamylation. Incubation of SAL with PNPBC resulted in similar curves, albeit with lower rates (data not shown). From these results we conclude that carbamates are useful substrate analogs to study the acylation and deacylation steps of enzymatic ester hydrolysis.

To study the pH-dependence of the acylation and deacylation steps separately we used PNPBC. The specificity constant of carbamylation (k_c/K_C) was determined by measuring the carbamylation rate constant (k_c^{obs}) at varying concentrations of PNPBC. For SHL the rate of reaction over the pH range from 5.5 to 8 is faster than spontaneous hydrolysis of PNPBC and therefore we used SHL rather than the slower reacting SAL for these experiments. It appeared that the carbamylation of SHL with PNPBC is strongly pH-dependent, and a sigmoidally shaped curve was obtained (Figure 3). It was estimated that a group with a pK_a around 7 controls the carbamylation reaction. The increase in specificity constant at higher pH results from an increase in both the carbamylation rate (higher k_c) and an increased affinity for the carbamate (lower K_C). For example, when the pH is raised from 6 to 7 the value of k_c increases from 9.1×10^{-3} to 29.8×10^{-3} s^{-1} and K_C changes from 120 to

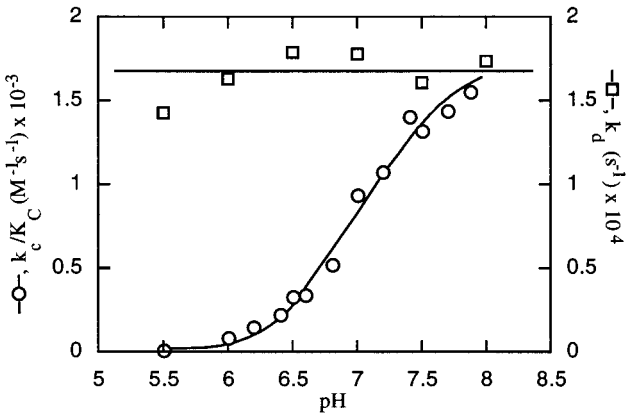

FIGURE 3: pH profiles of carbamylation (○) and decarbamylation (□) for SHL. The reactions were performed in 50 mM buffer, 10 mM $CaCl_2$, and 0.5 mg/mL BSA at 18 °C. The specificity constants for carbamylation and rate constants for decarbamylation were obtained as described in the text.

Table 2: Specificity Constants for Carbamylation of SHL and SAL with Different Chain Length *p*-Nitrophenyl *N*-Alkylcarbamates[a]

	k_c/K_C (M^{-1} s^{-1})	
carbamate	SHL	SAL
PNPEC	314[b]	35[b]
PNPBC	930[b]	9[b]
PNPOC	31 200[c]	*d*
PNPDC	11 600[c]	*d*

[a] Inhibitions were performed in 50 mM Hepes, pH 7, 10 mM $CaCl_2$, and 0.5 mg/mL BSA at 18 °C. [b] k_c^{obs} values obtained by the discontinuous approach were plotted against the concentration of carbamate, and k_c/K_C was calculated from the linear portion of this plot. [c] As for *b* but now the continuous approach was used. [d] The very low rates of carbamylation for SAL with these long chain carbamates did not allow an accurate determination of the specificity constants.

32 μM. To determine decarbamylation rates we carbamylated SHL on a preparative scale and isolated it as described in Materials and Methods. Subsequently the carbamyl-enzyme was incubated at varying pH values and recovery of activity was followed in time. Between pH 5.5 and 8 the decarbamylation rate is within experimental error independent of pH (Figure 3).

The chain length selectivity of SHL and SAL was studied with carbamates of different chain lengths. The reactions were all performed at pH 7 in the presence of 10 mM $CaCl_2$ and 0.5 mg/mL BSA. A neutral pH was chosen because under these conditions both SHL and SAL have a high reactivity while the carbamates have a good chemical stability. SHL is rapidly inhibited by PNPEC: if the enzyme is incubated with a 20 μM solution of PNPEC a half-time of inactivation of 2 min is observed. If the chain length of the carbamate is increased to eight carbon atoms as in PNPOC, the specificity constant of SHL increases 100-fold and remains high even with the dodecyl compound PNPDC (Table 2). The carbamylation of SAL is at least 9-fold slower than that of SHL (Table 2), and in sharp contrast to the behavior of SHL the specificity constant for SAL decreases upon increasing the chain length of the carbamate. As a result the specificity constant of SAL for PNPBC could still be measured, but the carbamylation rates with the long chain carbamates PNPOC and PNPDC are too slow to be determined.

To study the decarbamylation more accurately, both SHL and SAL were isolated after preparative carbamylation with

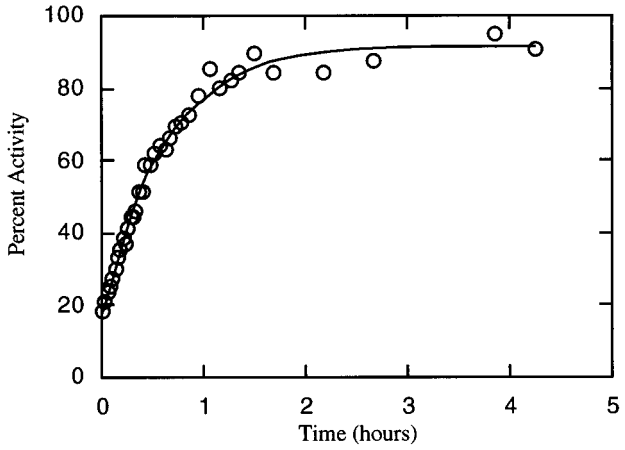

FIGURE 4: Decarbamylation of EC-SHL. Preparative carbamylation and isolation of the carbamyl-lipase were done as described in Materials and Methods. The reaction conditions for decarbamylation were 50 mM Hepes, pH 7, 10 mM $CaCl_2$, and 0.5 mg/mL BSA at 18 °C. Percent activities were determined on the basis of the OD_{280} of carbamylated enzyme and the specific activity of unmodified SHL.

Table 3: Decarbamylation Rates of SHL and SAL in the Absence and Presence of TX100[a]

	SHL		SAL	
carbamyl-enzyme	$10^4\ k_d$ (s^{-1}) no detergent	$10^4\ k_d$* (s^{-1}) 100 mM TX100	$10^4\ k_d$ (s^{-1}) no detergent	$10^4\ k_d$* (s^{-1}) 100 mM TX100
ethyl	4.5	10.4	0.32	0.88
butyl	1.7	9.2	0.30	1.11
octyl	1.0	2.0	ND	ND
dodecyl	4.4	2.2	ND	ND

[a] SHL and SAL were carbamylated on a preparative scale and the carbamyl-lipases were isolated as described in the experimental section. Decarbamylations were performed in 50 mM Hepes, pH 7, 10 mM $CaCl_2$, and 0.5 mg/mL BSA at 18 °C, either in the absence of detergent or in the presence of 100 mM detergent. ND = not determined.

carbamates of different chain length. At the start of the experiment about 15% activity is found because slow decarbamylation takes place during isolation and storage (see Materials and Methods). Upon incubation the activity gradually returns and within a few hours activity is almost completely recovered. In Figure 4 the decarbamylation profile of SHL after reaction with PNPEC is given, from which a first-order rate constant for decarbamylation (k_d) of $4.5 \times 10^{-4}\ s^{-1}$ was calculated. The decarbamylation curves for SHL after inhibition with PNPBC, PNPOC, and PNPDC are similar (not shown), and the corresponding k_d values are given in Table 3. Decarbamylation of SAL is about 10 times slower than decarbamylation of SHL, and the decarbamylation rate hardly depends on chain length.

Because interfaces influence the kinetic behavior of lipases, we tested the effect of TX100 on carbamylation. To this end we used PNPBC because it has a low solubility in water, a good miscibility with micelles, and a good reactivity with both SHL and SAL. The solubility of PNPBC is still sufficient to determine inactivation rates (k_c^{obs}) as a function of its concentration in the monomeric region in the absence of detergent. The results for SAL and SHL are depicted in Figures 5A and 5B, respectively. The maximum carbamylation rates (k_c) were determined by fitting the data to the equation $k_c^{obs} = k_c C/K_C + C$ as described in Materials and Methods. From the curves in Figure 5 maximum carbamylation rates of $1.4 \times 10^{-3}\ s^{-1}$ for SAL and $30 \times 10^{-3}\ s^{-1}$ for SHL and K_C values of 160 μM (SAL) and 30 μM (SHL) were calculated. In the previous experiments we used monomolecular inhibitor solutions. To study the influence of interfaces it is important to choose conditions where all enzyme is present in the bound form (E* in Scheme 1). In a previous article we showed that in the presence of 100 mM TX100 all SHL or SAL is present in the interface as E* (*14*). Therefore we used a fixed concentration of 100 mM TX100 and we varied the mole percentage of PNPBC in the interface from 0 to 0.2. The presence of TX100 only has a minor effect on the carbamylation rate of SAL (Figure 5A), and a k_c* of $2.3 \times 10^{-3}\ s^{-1}$ and a K_C* value of 0.2 mol % were obtained. For SHL the rate of inhibition increased linearly with the mole fraction PNPBC, indicating that in this (two-dimensional) concentration range SHL cannot be saturated with carbamate (Figure 5B) and hence the maximal rate of inactivation cannot be calculated. Although this observation makes a quantitative estimate impossible, Figures 5A and 5B clearly show that the presence of detergent dramatically enhances the reactivity of SHL whereas it hardly

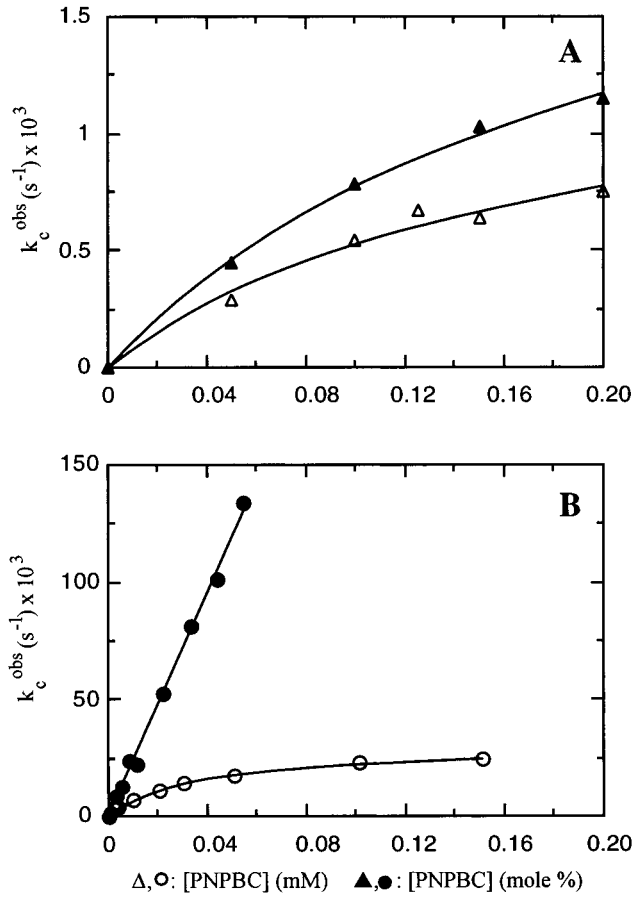

FIGURE 5: Carbamylation rates of SAL and SHL at different concentrations of carbamate in the absence and presence of an interface. SAL (panel A) was carbamylated with increasing concentrations of PNPBC in buffer (open symbols) or in the presence of a fixed concentration (100 mM) of TX100 (closed symbols). In the first case the carbamate concentration is expressed in mM; in the second case as mole percentage relative to TX100. Carbamylation reactions took place in 50 mM Hepes, pH 7, 10 mM $CaCl_2$, and 0.5 mg/mL BSA at 18 °C. For SHL (panel B) the conditions were identical. The observed rate constants for carbamylation, k_c^{obs}, at the different carbamate concentrations were obtained by fitting curves of percent activity versus time to eq 3. Note the difference in scaling for the *Y*-axes.

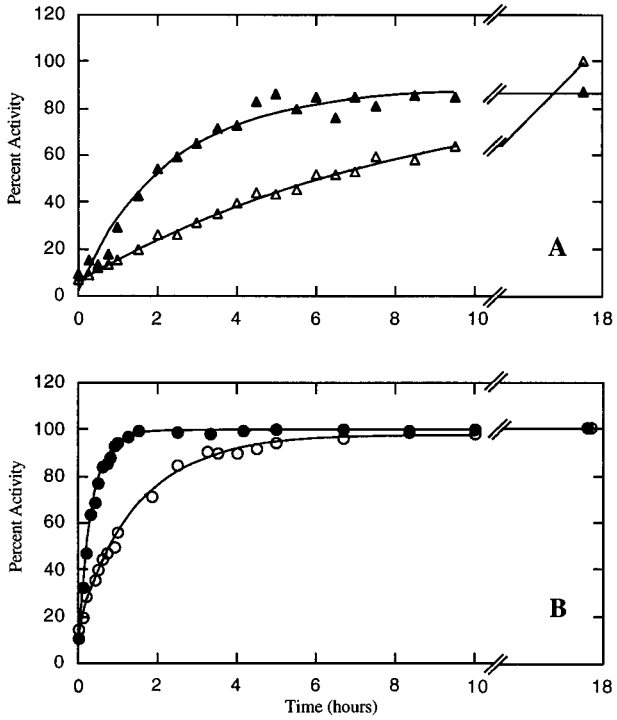

FIGURE 6: Decarbamylation of BC-SAL and BC-SHL in the absence and presence of an interface. Preparative carbamylation and isolation of the carbamyl-lipases was done as described in the experimental section. Decarbamylation of SAL (panel A) was performed in the absence (open symbols) and presence (closed symbols) of 100 mM TX100 in 50 mM Hepes, pH 7, 10 mM $CaCl_2$, and 0.5 mg/mL BSA at 18 °C. For SHL (panel B) the conditions were identical. Percent activities were determined on the basis of the OD_{280} of carbamylated enzyme and the specific activity of unmodified enzyme.

does so for SAL. Despite the observed rate enhancements, an exact interpretation of the magnitude of the change in the kinetic constants is hampered by the fact that concentrations have to be expressed in a three-dimensional way for monomeric substrates and in a two-dimensional way when an interface is present.

After we determined the effect of detergents on the carbamylation, we studied the effect of micelles on the kinetics of decarbamylation for different carbamates. The decarbamylation reaction is a first-order process quantified with the rate constant k_d (Scheme 2). In the presence of 100 mM TX100 the interfacially bound enzyme is defined as E* (Scheme 1), and hence we defined the interfacial rate constant of decarbamylation as k_d*. From Figures 6A and 6B it is clear that the decarbamylation rates of both BC-SAL and BC-SHL are enhanced by the presence of TX100 micelles. The rate enhancement for BC-SHL is slightly higher compared to the rate enhancement of BC-SAL. For SHL we also carried out these experiments with carbamates of longer chain lengths. Fitting of these curves yields k_d* values which are summarized in Table 3. The decomposition of the ethyl and butyl derivatives of SHL is clearly enhanced by Triton X100, but interestingly this activation effect of TX100 is lost if the chain length of the carbamate is increased (Table 3).

We used SHL to investigate the influence of detergent concentration on decarbamylation as well as to test the influence of other detergents than TX100. First, we determined the decarbamylation rate as a function of the TX100 concentration. In the absence of TX100 the decarbamylation

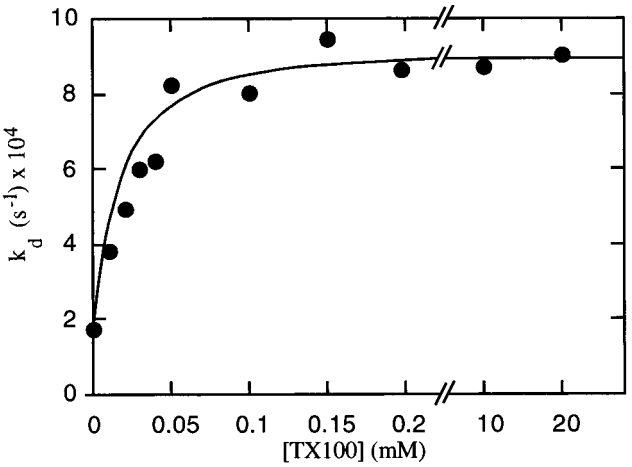

FIGURE 7: Decarbamylation rates of BC-SHL (0.15 μM) at varying concentrations of TX100. Conditions for decarbamylation are given in the legend of Figure 4.

Table 4: Effect of Detergents on the Decarbamylation Rate of BC-SHL[a]

detergent	$10^4\ k_d$(*) (s^{-1})	$t_{1/2}$ (min)
none	1.74	60
TX100	9.10	12
OPOE	8.44	13
$C_{18:1}$-PN	4.16	26
TDOC	3.83	29

[a] SHL was carbamylated on a preparative scale with PNPBC, and the carbamyl-lipase was isolated as described in Materials and Methods. The decarbamylation conditions are given in the legend of Table 3, but the detergent concentrations were 10 instead of 100 mM.

of BC-SHL is slow, and, as can be seen in Figure 7, upon addition of TX100 a continuous curve is obtained which levels off around a value of 9×10^{-4} s^{-1}. The critical micelle concentration (CMC) of TX100 is 0.25 mM (*27*). Surprisingly, already below the CMC of the detergent the maximum rate enhancement was reached. These data suggest that either monomeric TX100 can activate SHL or that TX100 can induce the formation of enzyme−detergent aggregates. "Premicellar aggregation" has been extensively demonstrated before for PLA_2 (*28*,*29*), but for lipases thus far little experimental support was found (*30*). We also studied the effect of other detergents on the decarbamylation rate of SHL. The detergents tested were neutral (OPOE), anionic (TDOC), and zwitterionic ($C_{18:1}$-PN), each at a concentration of 10 mM, which is at least two times their respective CMC values. In a separate experiment we verified that SHL is not inactivated by these detergents. The decarbamylation curves obeyed first-order kinetics and yielded complete recovery of activity, showing the enzyme stability in the presence of detergent once more. From the values presented in Table 4, it is obvious that these four detergents enhance the rate of decarbamylation. This enhancement is dependent on the type of detergent added, and a maximum activation effect of about a factor 5 was seen for the neutral detergents TX100 and OPOE.

Since Ca^{2+} is a cofactor of both SHL and SAL, it was of interest to test the influence of this ion on both the carbamylation and decarbamylation rates. From the data presented in Table 5 it is evident that for SHL the presence of calcium increases the carbamylation specificity constant k_c/K_C by a factor of 4. This effect can be mainly attributed

Table 5: Effect of Divalent Cations on Carbamylation and Decarbamylation Rate Constants of SHL with PNPBC[a]

	carbamylation			decarbamylation	
	k_c/K_C (M^{-1} s^{-1})	K_C (μM)	10^4 k_c (s^{-1})	10^4 k_d (s^{-1})	recovery (%)
calcium	930	32	300	1.74	100
EDTA	250	18	45	1.89	40
strontium	878	49	430	1.81	100

[a] Experiments were performed in 50 mM Hepes, pH 7, 0.5 mg/mL BSA at 18 °C in the absence of detergent. Calcium, EDTA, or strontium was present at a concentration of 10 mM. Further details are described in Materials and Methods.

to the 7-fold increase in k_c, whereas the affinity (K_C) for PNPBC in the presence of calcium is slightly lower. Calcium ions did not influence the rate of decarbamylation, although the recovery of active enzyme is decreased from 100% in the presence of calcium to 40% without calcium. It was shown before that strontium is the only divalent cation that can replace calcium with full retention of enzymatic activity (*31*). From the data in Table 5 it is clear that also for the carbamylation and the decarbamylation reactions strontium can replace calcium without significant changes in kinetic constants. For SAL not only strontium, but also barium can replace calcium with retention of activity (*14*). In line with that observation, the decarbamylation of SAL in the presence of calcium, strontium and barium gives comparable decarbamylation rates ($k_d = 0.3 \times 10^{-4}$ s^{-1}) and complete recovery of activity. Addition of EDTA resulted in a recovery of SAL activity as low as 5−10% (data not shown).

The fact that the carbamylation and decarbamylation rates are affected to only a minor extent by calcium indicates that Ca^{2+} ions are not directly involved in the bond breaking/bond making steps of the catalytic mechanism. Structural instability of the carbamylated (and possibly the acylated) enzymes in the absence of Ca^{2+} ions is suggested by the fact that the recovery of active SHL is reduced and the fact that the recovery of active SAL is almost completely lost in the absence of calcium. In this respect it is important to stress that during the catalytic cycle the acylated lipase is present at the interface. Therefore we investigated in more detail the influence of TX100 micelles on the decarbamylation. In the presence of Ca^{2+} ions, but in the absence of TX100, both SHL and SAL completely recover activity in decarbamylation experiments (Figures 6A and 6B). In the presence of TX100 and calcium ions, both lipases behave differently: whereas SHL again recovers complete activity, SAL activity levels off around 80%, both for PNPEC-inhibited (not shown) and PNPBC-inhibited SAL (Figure 6A). In the presence of 100 mM TX100 we found a

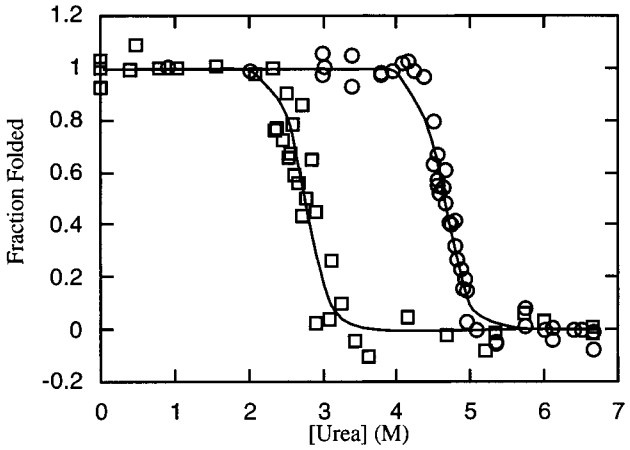

FIGURE 8: Urea-induced unfolding of SHL. The experiments were performed in the presence of 10 mM $CaCl_2$ (○) or in the presence of 10 mM EDTA (□). The SHL concentration was 0.3 μM in 50 mM Hepes, pH 7, at 18 °C.

complete recovery of BC-SHL activity not only in the presence but also in the absence of Ca^{2+}. In contrast, BC-SAL recovered only around 5% activity in the absence of calcium when TX100 is present (data not shown). These results show that Ca^{2+} ions have a stabilizing effect on both SAL and SHL. However, TX100 micelles stabilize SHL but destabilize SAL, an observation that is surprising for two quite homologous lipolytic enzymes.

The results presented above suggest that calcium is very important for the structure and stability of SAL and SHL. This finding was further investigated with denaturation studies in the presence and absence of calcium. Upon unfolding of SHL with urea the fluorescence quantum yield decreases about 2-fold. Both in the presence and absence of calcium the unfolding proceeds as a single transition over a narrow urea concentration range, indicating that the unfolding can be described as a two-state process. From Figure 8 it follows that calcium indeed has a profound effect on the stability of SHL. The midpoint of unfolding is shifted from 4.6 M urea in the presence of calcium to 2.8 M urea in the absence of calcium and the removal of calcium changes the ΔG_0 value of unfolding from 12.0 kcal/mol in the presence of calcium to 5.7 kcal/mol in the absence of calcium. For SAL an even bigger change in ΔG_0 upon removal of calcium is observed (Table 6), which can be attributed mainly to an almost 5-fold decrease in the slope (m) of the denaturation curve.

Our observations that the rate of decarbamylation is independent of the presence of calcium, whereas the percentage of recovery is calcium-dependent, suggest that also for the carbamylated enzyme calcium plays an important structural role. A technical complication in unfolding studies with

Table 6: Parameters Characterizing the Urea Unfolding of Unmodified and Sulfonylated SHL and SAL[a]

	10 mM calcium			10 mM EDTA		
protein	ΔG_0 (kcal/mol)	m (kcal/mol M)	$[\text{urea}]_{1/2}$ (M)	ΔG_0 (kcal/mol)	m (kcal/mol M)	$[\text{urea}]_{1/2}$ (M)
SHL	12.0	2.6	4.6	5.7	2.0	2.8
BS-SHL[b]	10.2	2.2	4.6	2.0	0.77	2.6
SAL	15.0	3.6	4.2	1.6	0.84	1.9
BS-SAL[b]	8.5	2.2	3.8	1.3	1.18	1.1

[a] Measured in 50 mM Hepes at pH 7 and 18 °C. The parameters were determined as described in Materials and Methods. $[\text{urea}]_{1/2} = \Delta G_0/m$ represents the midpoint of the urea unfolding curve. [b] Sulfonylated enzymes were prepared as described in Materials and Methods.

carbamylated enzyme is the fact that the carbamylated lipase is not stable, and, as a result, the percentage unmodified lipase will increase during the time course of the experiment. To overcome this problem we used sulfonylated SAL and SHL, which mimic the transition state of acyl enzyme hydrolysis, but in contrast to the carbamylated lipases are irreversibly inhibited. The first interesting observation is that for both lipases the sulfonylated forms are less stable than the unmodified lipases (see Table 6). Furthermore it is obvious that calcium also is important for the structural stabilization of the sulfonylated enzymes, since both ΔG_0 and the midpoints of unfolding are lowered upon changing from saturating (10 mM) calcium to the absence (EDTA) of calcium ions.

DISCUSSION

Comparative characterisation of the structurally highly similar lipases SAL and SHL revealed important functional differences (*14*). The results can be summarized as follows. SAL displays a pH optimum of 6.5, a $K_{Ca^{2+}}$ of 250 μM, a strong preference for acyl chains of 4 carbon atoms and hydrolyzes neutral glycerides but not phospholipids. In contrast SHL has a pH optimum of 8.5, a $K_{Ca^{2+}}$ of 15 μM and is less sensitive to changes in acyl chain length. It has high lipase activity (5−10 times higher than SAL) and an even higher phospholipase activity. Acyl *p*-nitrophenyl esters are good substrates for both SHL and SAL, but the two-step mechanism of hydrolysis of these esters by both lipases does not show "burst" kinetics. This leaves us with two possibilities: (i) the acylation step and not the deacylation step is rate-limiting, and (ii) the deacylation step is rate-limiting but both the acylation and deacylation are very fast. In either case it is difficult, if not impossible, to isolate the acylated enzyme to study this two-step reaction in more detail. To understand the kinetic differences between both enzymes, their reactions with the structurally related *p*-nitrophenyl *N*-alkylcarbamates were studied in detail. With these carbamates the second-order carbamylation rates (k_c/K_C) are 10−1000 times slower compared to the acylation reaction (k_{cat}/K_M) with the PNPB ester. The decarbamylation rates are 5 orders of magnitude smaller than k_{cat} for PNPB turnover. This slow turnover of the carbamyl-enzymes enables their isolation, giving the possibility to study both steps of the reaction separately.

To study the strong pH-dependence of these lipases we used PNPBC as a substrate mimic. The decarbamylation reaction clearly is pH-independent, which might be caused by the presence of a hydrogen bond between the amide function in the carbamate and the active site histidine, as suggested before by Shin and Quinn (*20*). Activation of a water molecule by the histidine is impaired and decarbamylation probably results from direct nucleophilic attack by a water molecule, which explains the pH independence and the low rate of the decarbamylation step. In contrast, the carbamylation reaction is strongly dependent on the pH and the obtained pH profile with a pK_a around 7 probably represents the titration of the active site histidine. Our results show that the pH dependence resides in the carbamylation step.

The inhibition of both SAL and SHL by PNPBC follows saturation kinetics and allows determination of the rate constants K_C and k_c, which are analoguous to K_M and k_{cat} for acylation/deacylation. The higher reactivity of SHL (k_c/K_C = 930 M^{-1} s^{-1}) compared to SAL (k_c/K_C = 9 M^{-1} s^{-1}) with this carbamate can be attributed mainly to the more than 20-fold increase in k_c, which is in good agreement with the difference in k_{cat} between SHL and SAL with the corresponding ester (*14*). Furthermore there is a difference between both enzymes in affinity for PNPBC of a factor 5. In good agreement with the strong preference for small substrates of SAL, inhibition by the shorter carbamate PNPEC is more efficient and upon increasing the chain length of the carbamate, the reactivity of SAL decreases dramatically. SHL has a preference for longer chains, and an optimum carbamylation rate was found for PNPOC. Because no saturation kinetics were observed for the long chain carbamates, it is difficult to attribute this higher reactivity of SHL with longer inhibitors to either reactivity (k_c) or affinity (K_C). Because of the magnitude of increase in k_c/K_C for longer chains (30−100-fold), this increase cannot result solely from a decrease in K_C, which should have resulted in saturation kinetics. Therefore this high reactivity with longer chains is mainly the result of an increase in k_c. The use of the binding energy of larger substrates to increase k_{cat} rather than to decrease K_M has also been described for a number of proteases (*32*).

In summary, the result of increasing the alkyl chain length on the catalytic power of both lipases is significant and in opposite direction: SHL reactivity increases upon increasing the chain length with an optimum reactivity for the octylcarbamate, whereas SAL reactivity is lost almost completely for the medium and long chain carbamates. In our opinion these large differences cannot be explained by small chemical changes of the cleavable bond due to an increase in chain length. The differences in chain length selectivity between both lipases could, however, very well result from differences in the sizes of the acyl binding pockets, comparable to the situation described recently for several mutants of the lipase from *Rhizopus delemar* (*33*). If so, than SAL would have a restricted, small acyl binding pocket that prevents larger substrates to bind, or allows binding, but not in such a manner that the ester bond is in optimal orientation for catalysis. In contrast, SHL would have a more extended and/or flexible binding pocket permitting also the binding of medium to long chains. Another possibility is that both lipases differ in the way and in the extent in which they interact with the substrate interface. That there are important differences between SHL and SAL at this level of enzyme−substrate interaction is clearly shown by us in this study (e.g. Figure 5). Because the three-dimensional structures of SHL and SAL are not available yet, it is impossible at this moment to address the difference in chain length selectivity between both lipases to either of these options. In contrast to the carbamylation reaction, the decarbamylation rates for both SHL and SAL only slightly depend on chain length. On the basis of these findings we therefore conclude that the difference in chain length selectivity between both enzymes is expressed during carbamylation, which corresponds to the acylation step in ester hydrolysis.

The decarbamylation rate of SAL and SHL is enhanced three to 5-fold upon addition of micelles, which strongly suggests a direct effect on catalytic activity in the decarbamylation. How do we explain this similar behavior of SAL and SHL in the decarbamylation step, where the effect of micelles in the carbamylation step is that pronounced for

SHL and almost absent for SAL? In most lipase structures a lid has been identified that blocks the active site, but moves away upon interfacial or substrate binding (see ref *34*, and references therein). On the basis of inactivation experiments with hexadecylsulfonyl fluoride incorporated in TX100 micelles, it was concluded that SHL also has a lid (*15*). That SAL lacks a lid and has an exposed active site is unlikely for two reasons. Firstly, the primary structures of SAL and SHL show high sequence homology, and no deletions are present that suggest the absence of a lid in SAL. Secondly, the effect of TX100 in the decarbamylation step of SAL indicates that conformational changes take place upon micellar binding/interaction. The absence of a rate enhancement in the carbamylation step for SAL might, however, be explained by a difference in the flap region. As discussed before by Rubin (*35*), the model of a lipase existing either in the closed or in the open conformation is probably too simple, and a whole range of intermediate conformations that are in equilibrium should be considered. Possibly for SHL the equilibrium is shifted more easily toward the open, activated conformation than for SAL.

In a paper describing the kinetics of lipoprotein lipase with carbamates, Shin and Quinn predicted a larger effect by the addition of micelles on the hydrolysis of carbamyl-lipases inhibited by longer chains (*20*). This is the opposite of what we have found experimentally. Because of the absence of a rate enhancement of SHL after inhibition with the dodecyl carbamate, it is tempting to conclude that binding of the longer chain yields an activated (open form) conformation. We suggest that a short chain lipid binds in the active site with minor conformational changes, but after introduction of the chain the enzyme may return to the closed form. In that case addition of an interface would result in the generation of the activated form. Therefore, an effect by micelles on the decarbamylation rate will only be observed with short acyl chains.

Many enzymes use metal ions as cofactors for either their structural stabilization, or in the catalytic mechanism, or in a combination of both functions. An example of an enzyme that is dependent on calcium for its catalytic activity is PLA_2, and for this enzyme the calcium ion is directly involved in the catalytic mechanism (*36*). Both SHL and SAL also need calcium for full catalytic activity, but it has been suggested that the role of calcium in these lipases is structural rather than mechanistic (*14*,*15*,*31*). Our kinetic studies with carbamates support this proposal of a structural function and therefore we further investigated the importance of calcium for the structure of these proteins with urea unfolding experiments. The native state of many proteins can be demonstrated to exist in a dynamic equilibrium with an alternative, less structured state known as the unfolded or denaturated state. The equilibrium constant for this reversible reaction is determined by the free energy difference ΔG_0 between these two states. For almost all of the proteins that have been studied the ΔG_0 of unfolding ranges between 5 and 15 kcal/mol (*37*). The finding that the ΔG_0 of unfolding in the presence of calcium is 12 kcal/mol for SHL and 15 kcal/mol for SAL shows that both lipases are very stable proteins in the presence of their cofactor. Upon removal of calcium the ΔG_0 values, however, drastically decrease, which is direct proof for a structural stabilization by the cofactor calcium for both SHL and SAL. This lower stability results not only from a shift in the midpoint of unfolding but also from a decrease in the slope of the unfolding curves. This latter phenomenon has been observed for other proteins as well, and it has been suggested that it results from the presence of more unfolding intermediates in the unfolding pathway (*38*−*40*). An alternative explanation for the lower *m* values in the absence of calcium is that the lipases are already partially unfolded in the absence of their cofactor. As a consequence the amount of hydrophobic area which becomes exposed upon unfolding is lower resulting in a lower *m* value. We also studied the stability of sulfonylated SHL and SAL, which mimic the acylated enzymes. These sulfonylated enzymes are less stable than the unmodified forms, both in the absence and presence of calcium. This observation is in contrast to the general notion that enzymes are stabilized by the presence of substrate or a substrate mimic. If SHL and SAL are saturated with substrate, they will quickly react and form acylated enzymes with a subsequent loss in stability. For these lipases the concept of "substrate stabilization" apparently does not apply.

Although both SAL and SHL have been classified as true lipases (*41*), we showed that only SHL can hydrolyze long chain substrates (this study and ref 14). One criterion to classify an esterase as a member of the subfamily of lipases is the capacity to degrade long chain triacylglycerols (*42*). Obviously, SAL does not match this criterion. Another criterion commonly used is to ascertain whether the enzyme in question displays interfacial activation. The disadvantage of this approach is that assays to measure interfacial activation are subject to numerous artefacts and therefore are unreliable (*43*). Our results with carbamates, however, clearly show that SHL activity is enhanced upon addition of micelles and that this effect is most pronounced in the first step of the reaction. Therefore our results justify the previous classification of SHL as a true lipase with broad substrate specificity. In sharp contrast the carbamylation rate of SAL hardly increases in the presence of an interface. Again, classification of SAL as a true lipase does not seem to be justified. We propose that SAL should be considered as an intermediate between an esterase and a true, interfacially activated lipase, together with other hydrolases such as the *Candida antarctica* B lipase (*44*) and cutinase (*45*). In this respect, SAL and SHL provide an unique system to study the (evolutionary) bridging between esterases and lipases.

ACKNOWLEDGMENT

The authors thank Jacco van Alphen, Ruud Cox, and Daniel Nagore for the assistance in experimental work and fruitfull discussions, Cécile Lemette for secretarial help, and Ingrid van Rooijen for help in preparing the figures.

REFERENCES

1. Brockerhoff, H., and Jensen, R. G. (1974) *Lipolytic Enzymes*, Academic Press, New York.
2. Sarda, L., and Desnuelle, P. (1958) *Biochim. Biophys. Acta 30*, 513−521.
3. Verger, R., and de Haas, G. H. (1976) *Annu. Rev. Biophys. Bioeng. 5*, 77−117.
4. Volwerk, J. J., and de Haas, G. H. (1982) in *Molecular Biology of Lipid−Protein Interactions* (Griffith, O. H., and Jost, P. C. Eds.) Wiley, New York.

5. van den Berg, B., Tessari, M., Boelens, R., Dijkman, R., de Haas, G. H., Kaptein, R., and Verheij, H. M. (1995) *Nat. Struct. Biol. 2*, 402−406.
6. Winkler, F. K., D'Arcy, A., and Hunziker, W. (1990) *Nature 343*, 771−774.
7. van Tilbeurgh, H., Egloff, M.-P., Martinez, C., Rugani, N., Verger, R., and Cambillau, C. (1993) *Nature 362*, 814−820.
8. Brzozowski, A. M., Derewenda, U., Derewenda, Z. S., Dodson, G. G., Lawson, D. M., Turkenburg, J. P., Bjorkling, F., Huge-Jensen, B., Patkar, S. A., and Thim, L. (1991) *Nature 351*, 491−494.
9. Egloff, M.-P., Marguet, F., Buono, G., Verger, R., Cambillau, C., and van Tilbeurgh, H. (1995) *Biochemistry 34*, 2751−2762.
10. Grochulski, P., Li, Y., Schrag, J. D., Bouthillier, F., Smith, P., Harrison, D., Rubin, B., and Cygler, M. (1993) *J. Biol. Chem. 268*, 12843−12847.
11. Hjorth, A., Carrière, F., Cudrey, C., Wöldike, H., Boel, E., Lawson, D. M., Ferrato, F., Cambillau, C., Dodson, G. G., Thim, L., and Verger, R. (1993) *Biochemistry 32*, 4702−4707.
12. Charton, E., and Macrae, A. R. (1992) *Biochim. Biophys. Acta 1123*, 59−64.
13. Bertolini, M. C., Schrag, J. D., Cygler, M., Ziomek, E., Thomas, D. Y., and Vernet, T. (1995) *Eur. J. Biochem. 228*, 863−869.
14. Simons, J. W. F. A., Adams, H., Cox, R. C., Dekker, N., Götz, F., Slotboom, A. J., and Verheij, H. M. (1996) *Eur. J. Biochem. 242*, 760−769.
15. Leuveling Tjeenk, M., Bulsink, Y. B. M., Slotboom, A. J., Verheij, H. M., de Haas, G. H., Demleitner, G., and Götz, F. (1994) *Protein Eng. 7*, 579−583.
16. Aldridge, W. N., and Reiner, E. (1972) *Enzyme Inhibitors as Substrates: Interaction of Esterases with Esters of Organophosphorus and Carbamic Acids*, North-Holland, Amsterdam.
17. Feaster, S. R., Lee, K., Baker, N., Hui, D. Y., and Quinn, D. M. (1996) *Biochemistry 35*, 16723−16734.
18. Fourneron, J.-D., Abouahil, N., Chaillan, C., and Lombardo, D. (1991) *Eur. J. Biochem. 196*, 295−303.
19. Scofield, R. E., Werner, R. P., and Wold, F. (1977) *Biochemistry 16*, 24923−2496.
20. Shin, H. C., and Quinn, D. M. (1992) *Biochemistry 31*, 811−818.
21. van Dam-Mieras, M. C. E., Slotboom, A. J., Pieterson, W. A., and de Haas, G. H. (1975) *Biochemistry 14*, 5387−5394.
22. Horrevoets, A. J. G., Verheij, H. M., and de Haas, G. H. (1991) *Eur. J. Biochem. 198*, 247−253.
23. Mach, H., Russel Middaugh, C., and Lewis, R. V. (1992) *Anal. biochem. 200*, 74−80.
24. Greenzaid, P., and Jencks, W. P. (1971) *Biochemistry 10*, 1210−1222.
25. Hosie, L., Sutton, L. D., and Quinn, D. M. (1987) *J. Biol. Chem. 262*, 260−264.
26. Pace, C. N. (1986) *Methods Enzymol. 131*, 266−280.
27. Mukerjee, P., and Mysels, K. L. (1971) *Critical Micelle Concentrations of Aqueous Surfactant Systems*, National Standard Reference Data Sereries, National Bureau of Standards, U.S. Government Printing Office, Washington, DC.
28. Deveer, A. M. Th.J., den Oude, A. T., Vincent, M., Gallay, J., Verger, R., Egmond, M. R., Verheij, H. M., and de Haas, G. H. (1992) *Biochim. Biophys. Acta 1126*, 95−104.
29. van Eijk, J. H., Verheij, H. M, Dijkman, R., and de Haas, G. H. (1983) *Eur. J. Biochem. 132*, 183−188.
30. Egmond, M. R. (1996) in *Engineering of/with Lipases* (Malcata, F. X., Ed.) pp 183−191, Kluwer Academic Publishers, Dordrecht.
31. van Oort, M. G., Deveer, A. M. Th. J., Dijkman, R., Leuveling Tjeenk, M., Verheij, H. M., de Haas, G. H., Wenzig, E., and Götz, F. (1989) *Biochemistry 28*, 9278−9285.
32. Fersht, A. (1985) *Enzyme Structure and Mechanism*, pp 311−346, W. H. Freeman and Company, New York.
33. Klein, R. R., King, G., Moreau, R. A., and Haas, M. J. (1997) *Lipids 32*, 123−130.
34. Schrag, J. D., Li, Y., Cygler, M., Lang, D., Burgdorf, T., Hecht, H. J., Schmid, R., Schomburg, D., Rydel, T. J., Oliver, J. D., Strickland, L. C., Dunaway, C. M., Larson, S., Day, J., and McPherson A. (1997) *Structure 5*, 187−202.
35. Rubin, B. (1994) *Nat. Struct. Biol. 1*, 568−572.
36. Verheij, H. M., Volwerk, J. J., Jansen, E. H. J. M., Puik, W. C., Dijkstra, B. W., and de Haas, G. H. (1980) *Biochemistry 19*, 743−750.
37. Privalov, P. L. (1979) *Adv. Protein Chem. 33*, 167−241.
38. Bai, Y., Sosnick, T. R., Mayne, L., and Englander, S. W. (1995) *Science 269*, 192−197.
39. Godbole, S., Dong, A., Garbin, K., and Bowler, B. E. (1997) *Biochemistry 36*, 119−129.
40. Shortle D., and Meeker, A. K. (1989) *Biochemistry 28*, 936−944.
41. Nikoleit, K., Rosenstein, R., Verheij, H. M., and Götz, F. (1995) *Eur. J. Biochem. 228*, 732−738.
42. Egloff, M. P., Ransac, S., Marguet, F., Rogalska, E., van Tilbeurgh, H., Buono, G., Cambillau, C., and Verger, R. (1995) *Ol., Corps Gras, Lipides 2*, 52−67.
43. Verger, R. (1997) *Trends Biotechnol. 15*, 32−38.
44. Uppenberg, J., Hansen, M. T., Patkar, S., and Jones, T. A. (1994) *Structure 2*, 293−308.
45. Martinez, C., De Geus, P., Lauwereys, M., Matthyssens, G., and Cambillau, C. (1992) *Nature 356*, 615−618.

BI9713714